Alan Connelly, PhD • Graeme D. Jackson, FRACP • Richard S. J. Frackowiak, MD
John W. Belliveau, PhD • Faraneh Vargha-Khadem, PhD • David G. Gadian, DPhil

Functional Mapping of Activated Human Primary Cortex with a Clinical MR Imaging System[1]

Functional activation of the human brain can be visualized with magnetic resonance (MR) imaging, but most studies so far have used echo-planar imaging or magnetic fields of 2 T and above, neither of which are at present widely available. The authors used a standard 1.5-T MR imaging system to map regions of the brain that are activated with visual and motor tasks, using a long echo time (60 msec) fast low-angle shot sequence. Eleven visual and 14 motor studies were performed, and activation was seen in all cases. Up to 15% signal intensity change was apparent in gray matter but not in white matter. The precise anatomic location and extent of activation were defined by reference to T1-weighted images acquired during the same examination. This method of relating brain structure to function uses equipment that is widely available, which has considerable implications for the investigation of many neurologic and neurosurgical diseases and for our understanding of brain function and dysfunction.

Index terms: Blood, flow dynamics • Brain, blood flow, 10.919 • Brain, function, 10.919 • Magnetic resonance (MR), vascular studies

Radiology 1993; 188:125–130

[1] From the Radiology and Physics Unit (A.C., D.G.G.) and Neurosciences Unit (G.D.J., F.V.K.), Institute of Child Health and Hospital for Sick Children, Great Ormond St, London WC1N 3JH, England; the Medical Research Council Cyclotron Unit and Institute of Neurology, London (R.S.J.F.); and the Department of Radiology, Massachusetts General Hospital, Charlestown, Mass (J.W.B.). From the 1992 RSNA scientific assembly. Received November 20, 1992; revision requested December 23; revision received January 20, 1993; accepted February 17. F.V.K. supported by the Medical Research Council; J.W.B. supported by the McDonnell-Pew Program in Cognitive Neuroscience. **Address reprint requests to** D.G.G.

RECENT developments in noninvasive imaging methods provide new opportunities for the investigation of human brain function. These methods of "functional brain mapping" rely on the visualization of local physiologic changes within the brain that are associated with activation of the visual, motor, or other brain systems. The technique that has so far contributed most to functional brain mapping is positron emission tomography (PET) (1,2). Observations made with PET (3,4) indicate that an increase in local venous blood oxygenation occurs with cerebral activation. Such an increase provides an explanation for the changes in water signal intensity that now form the basis of functional mapping with magnetic resonance (MR) imaging, as recently described (5–10). MR imaging has better spatial and temporal resolution than PET and does not use ionizing radiation. However, most of the functional MR imaging studies have so far involved the use of echo-planar "snapshot" imaging (11) or magnetic fields of 2 T and above, neither of which are at present widely available. In this report, we describe our initial experience with functional brain mapping using a conventional MR imaging system operating at 1.5 T in a diagnostic radiology department with a heavy service commitment. The quality of the activation maps that we obtained during visual and motor tasks suggests that functional MR imaging will find widespread application both in research and in more routine clinical investigations.

MATERIALS AND METHODS

MR imaging studies were carried out on a Siemens 1.5-T SP system (Siemens AG, Medical Group, Erlangen, Germany) with a standard circularly polarized head coil. Field homogeneity was adjusted by means of "global shimming" for each subject, with typical line widths for the global shimming being about 20 Hz. Sagittal, and in some cases coronal, multisection T1-weighted images were then obtained (repetition time msec/echo time [TE] msec = 600/15; 256 × 256 matrix; section thickness, 5 mm). With use of these images as an anatomic guide, appropriate tilted planes were selected for activation studies. These were as follows: (*a*) for visual stimulation, a tilted axial plane through the visual cortex, oriented along the line of the posterior limb of the calcarine sulcus (Fig 1a), and (*b*) for motor stimulation, one or more of the tilted axial planes through the primary motor and sensory cortex, as shown in Figure 1b–1d. The structural anatomy of these selected tilted planes was shown on T1-weighted images (600/15; 256 × 256 matrix; section thickness, 4–10 mm; field of view, 230 mm for the visual cortex and 170–230 mm for the motor studies). For the activation studies, the selected planes were then imaged by using a fast low-angle shot (FLASH) (12) sequence (72 or 85/60; pulse angle, 40°; 64 × 128 matrix), with the same field of view and section thickness as in the corresponding anatomic images. These sequence parameters were selected on the basis of the optimization studies described below. The section thickness was 8 mm for the visual activation studies; for the motor studies, it was 8–10 mm for the axial plane illustrated in Figure 1b and 4 mm for the axial planes seen in Figure 1c and 1d. The FLASH images were interpolated to and displayed as a 128 × 128 matrix. They were acquired in one or more series of up to 100 consecutive data acquisitions at intervals of about 9 or 10 seconds. This interval included 1.5 seconds of dead time, 1.5 seconds for eddy current stabilization, and 1 second for attainment of steady-state magnetization before acquisition. The images were then stored individually for subsequent analysis.

Visual activation was carried out by using light-proof stimulating goggles placed over the subject's eyes. Each eyepiece contained a single light-emitting diode. Five FLASH images were acquired with the

Abbreviations: FLASH = fast low-angle shot, PET = positron emission tomography, TE = echo time.

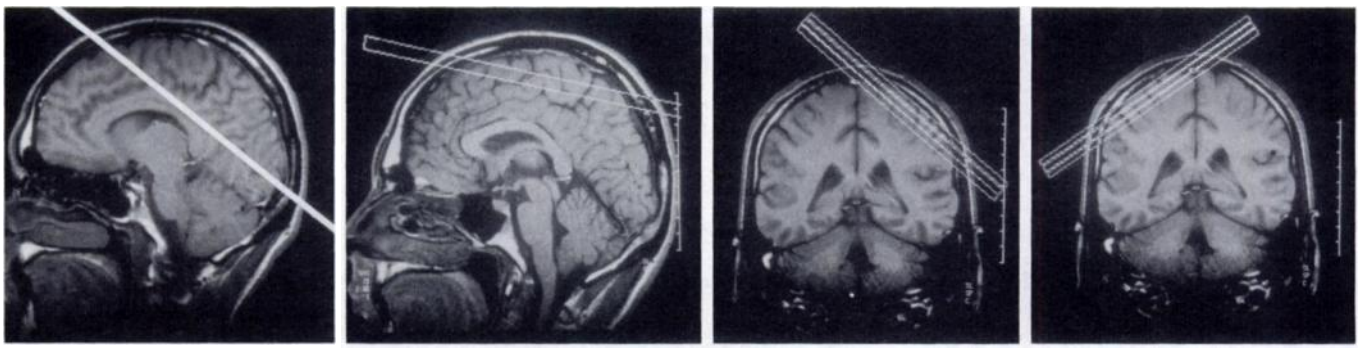

a. b. c. d.

Figure 1. Images illustrating the orientation of the axial planes selected for the visual studies **(a)** and the motor studies **(b–d)**. The plane in **b** was used for simultaneous examination of the left and right motor cortices, and the planes in **c** and **d** were selected for further investigations.

diodes off, then five more were acquired with the two diodes flashing synchronously at 8 Hz (5). This procedure was repeated 10 times, so that a total of 100 images were obtained over a period of 900 seconds. A total of 11 visual activation studies were carried out in six healthy volunteers (age range, 26–42 years). To optimize the acquisition parameters, images were obtained (*a*) with four different TEs (40, 60, 80, and 100 msec; repetition time = 92 or 112 msec) with a fixed pulse angle of 40° and (*b*) with four different pulse angles (20°, 40°, 60°, and 80°) at a fixed TE of 60 msec. These data, obtained from five subjects, formed the basis for selection of our routine data acquisition parameters.

The motor task consisted of repetitive finger-to-thumb opposition movements. In some studies, this involved sequential touching of the thumb with the first, second, third, and fourth fingers; in other studies, including those illustrated, all fingers were brought into contact with the thumb simultaneously. The rate and force of movement were not controlled. Data were collected in blocks of five control images followed by five obtained during motor activation. Initially, this procedure was repeated up to 20 times for each hand, but as our techniques improved, an adequate signal-to-noise ratio was achieved with as few as one to four repeats. A total of 14 motor activation studies were carried out in nine healthy volunteers (age range, 12–42 years).

Images were reconstructed in the standard manner. Activation images were obtained by subtracting sets of control images (ie, lights off or no finger movement) from those acquired during activation. No other postprocessing was carried out. To ensure that the images reflected steady-state conditions, the first image in each block of five (ie, the first image obtained on activation or deactivation) was omitted from the additions and subtractions; thus, the resulting activation images shown herein are derived from images 2–5 in each block of five images. Registration of activation and anatomic images was achieved by means of pixel-to-pixel identification of key features in the anatomic, control, and activation images. For the purposes of display, the activation images were then superimposed photographically on the anatomic images, with the key features used as reference points.

Signal intensities and activations are presented as means ± standard deviations.

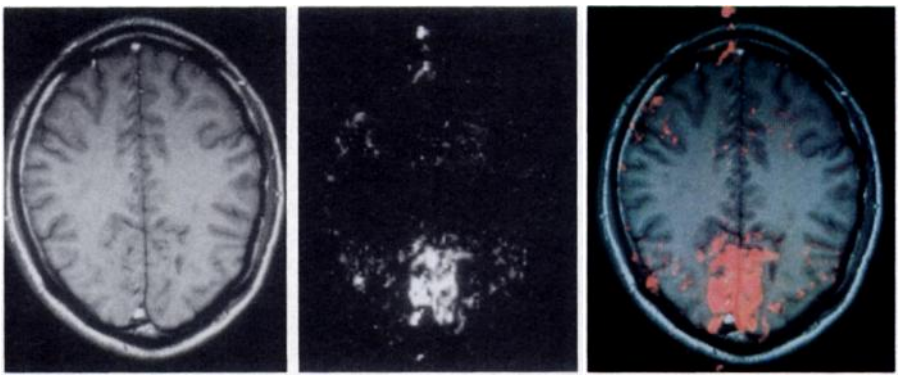

a. b. c.

Figure 2. Images from a study of visual activation, obtained with the section orientation shown in Figure 1a. **(a)** Anatomy of the selected section. **(b)** Effects of activation. This image was obtained by summing 40 FLASH images (72/60; pulse angle, 40°) acquired with the light-emitting diodes off (ie, 10 blocks of data, images 2–5 in each block) and subtracting the resulting image from the corresponding summation of images acquired with the diodes on. The total acquisition time for the image was 900 seconds. **(c)** Superimposition of **b** (in red) on **a**. The signal outside the brain in **b** and **c** is due to blood vessel pulsatility leading to "ghosting" in the phase-encoding direction. Such ghosts would not necessarily be reproducible from one image to another and can therefore appear as high signal intensity in a subtraction image.

RESULTS

Images from a study of visual activation are shown in Figure 2. The anatomy of the selected plane is displayed in Figure 2a, and the effects of activation are shown in Figure 2b. The image in Figure 2b was obtained by subtracting images acquired with the light-emitting diodes off from those acquired with the diodes on (see Materials and Methods and figure legend for more detail). Activated regions are visualized as areas of increased water signal intensity, this increase being attributed to a local change in blood oxygenation (3–8,13). Superimposition of Figure 2b on Figure 2a, as shown in Figure 2c, allows identification of the anatomic features that are activated.

With a view to optimizing the signal changes observed on activation, data were obtained from five subjects at four TE values and four pulse angles (see Materials and Methods). For each subject, analysis was based on a $9 \times 9 \times 8$-mm region of interest within the visual cortex that produced the greatest signal intensity increase on activation. At a fixed TE of 60 msec, the maximum signal intensity in the FLASH images and the subtraction images was obtained with 40° pulses. At a TE of 40 msec (with use of 40° pulses), the mean signal intensity increase on activation was 1.9% ± 0.3, in good agreement with the data of Kwong et al (5). The percentage increase varied approximately linearly with TE, reaching a value of 4.8% ± 1.7 at a TE of 100 msec. However, owing to T2* processes, the overall signal intensity in both the control and activated images declined with TE (T2* in

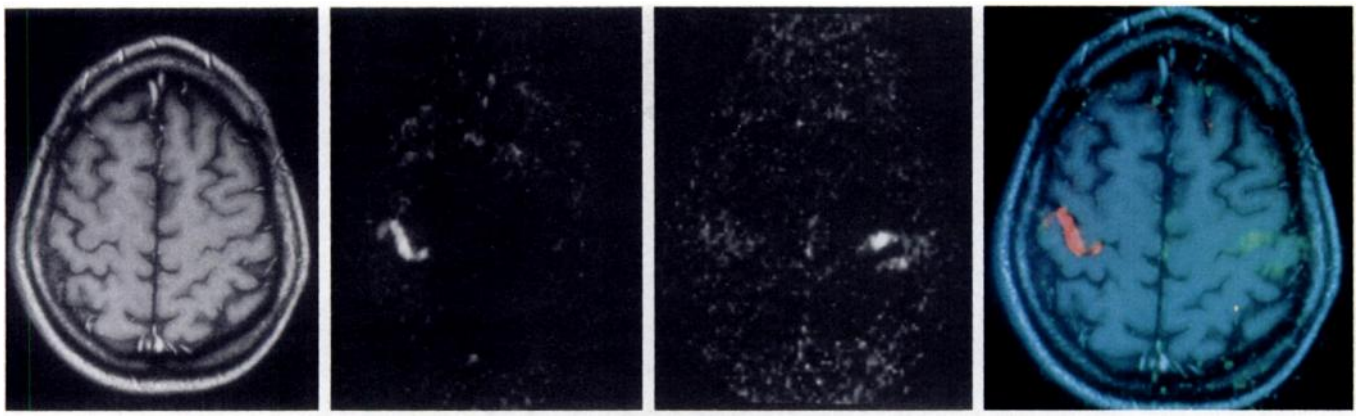

a. b. c. d.

Figure 3. Images from a study of motor stimulation involving a hand movement task, obtained with the section orientation shown in Figure 1b. **(a)** Anatomy of the selected section. **(b, c)** Effects of left hand **(b)** and right hand **(c)** movement. Both **b** and **c** were obtained by summing 80 FLASH images (ie, 20 blocks of data, images 2–5 in each block) acquired under control conditions (no movement) and subtracting the resulting image from the corresponding summation of images acquired during hand movement. The total acquisition time for **b** and **c** was 1,800 seconds each. (In subsequent examinations, adequate images could be obtained by using only five blocks of data.) For these images, parameters were 72/60; pulse angle, 40°; section thickness, 10 mm; and field of view, 230 mm. **(d)** Superimposition of **b** (in red) and **c** (in green) on **a.**

the activated region was 66 msec ± 8). It may readily be shown that on activation the maximum signal intensity increase in absolute terms can be expected at a TE value approximately equal to T2* (9). On the basis of these observations, a TE value of 60 msec with a pulse angle of 40° was selected for subsequent studies. These were the parameters used for the image shown in Figure 2b, in which the signal intensity increase on activation was 4.1%.

All 11 studies of visual stimulation showed activation, with a signal intensity increase at TE = 60 msec of 3.6% ± 1.5 (range, 2.0%–7.3%).

Figures 3–7 demonstrate the effects of motor activation, which involved the hand movement task described above. When the axial plane shown in Figure 3a was used, both left and right motor cortices were observed simultaneously. Figure 3b shows the effects of left hand movement and Figure 3c the effects of right hand movement. Appropriate cortical activity can be clearly seen in Figure 3b and 3c, the maximal signal intensity increase (based on a 5 × 5 × 10-mm region of interest) being 4.2% in the right motor cortex and 3.3% in the left. These values are representative of the activation (3.7% ± 1.4) measured in a total of 20 observations that were made with this axial plane. Figure 3d shows the superimposition of Figure 3b and 3c on the anatomic image shown in Figure 3a.

While the axial plane of Figure 3 is suitable for simultaneous examination of both left and right motor cortices, oblique planes through one hemisphere are preferable for viewing the detailed functional anatomy of the primary motor and sensory cortex. Therefore, further data were obtained with the planes shown in Figures 4 and 5. For these studies, the section thickness was reduced to 4 mm to minimize partial volume effects and the field of view was decreased to 170 mm. This produced an in-plane resolution of 2.6 × 1.3 mm, the interpolated voxel size in the displayed images being 1.3 × 1.3 × 4.0 mm.

As can be seen from the set of images shown in Figure 4, the distinction between gray and white matter during activation was apparent in these oblique sections. Activation can be seen in gray matter of the sulcal walls, with no apparent effect in the intervening white matter. For instance, the images in Figure 4b and 4c clearly show activation in the gray matter on both walls of the central sulcus. This particular set of images enables the activation to be related to the cortical surface as it would be seen at craniotomy. Furthermore, by following the activation down through successive sections, the region activated by the hand movement task can also be precisely defined and related to specific gyri and sulci at a deeper level. Figure 5 shows additional data obtained from the right hemisphere during left hand movement, again demonstrating that activation is observed only in the gray matter of the sulcal walls. The activated regions are consistent with the hand area of the motor and sensory cortex that would be expected to be activated by this task (14).

Each of the activation images shown in Figures 4 and 5 reflects a summation of data obtained over seven cycles of rest and activity. Therefore, accumulation of each data set lasted a total of 700 seconds. However, in many cases adequate images can be obtained in a shorter period; for instance, the activation in Figure 5b was observable after summing data from just one of the seven cycles, as shown in Figure 6. Figure 7 shows the cyclical signal intensity changes in a 3.9 × 2.6 × 4.0-mm volume of interest within the activated region shown in Figure 4b, the mean signal intensity increase in the seven cycles being 15.5% ± 3.1. In the same examination, the use of an imaging plane oriented as in Figure 1b, with a larger section thickness (8 mm vs 4 mm) and field of view (230 mm vs 170 mm), produced signal intensity increases of 3.5% in the right motor cortex and 4.4% in the left. The difference between the values of 4.4% and 15.5% presumably reflects the focal nature of the activation; this is best identified by the use of appropriately angled planes and reduced voxel size, resulting in a smaller partial volume effect.

DISCUSSION

The studies described above show that high-resolution images displaying the activated regions of the visual and sensorimotor cortices can be obtained with a conventional MR imager operating at 1.5 T. There are three main points that we wish to emphasize. First, the spatial resolution that we achieved for the motor studies (2.6 × 1.3 × 4.0 mm) enabled the anatomic location of the activated regions to be defined precisely. Second,

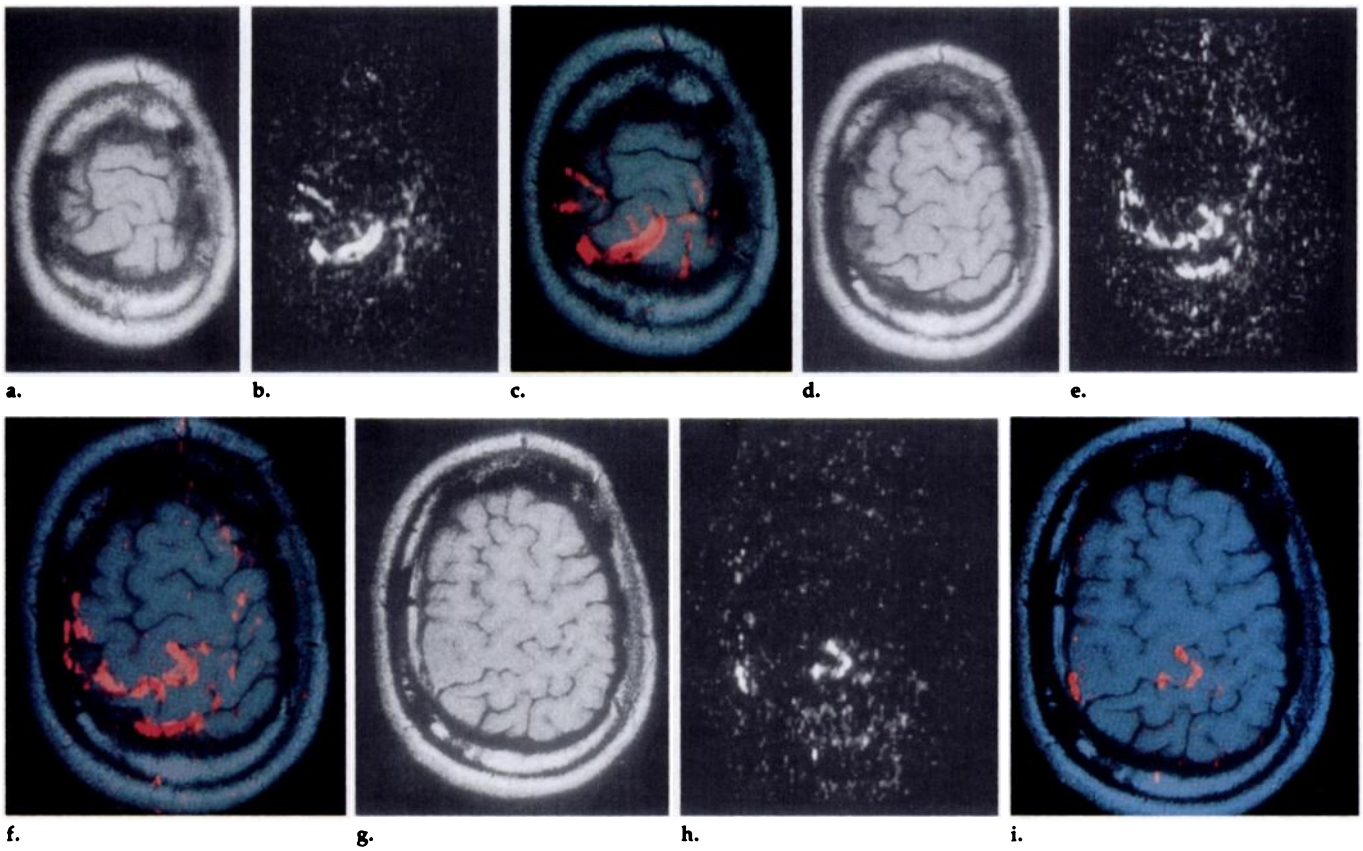

Figure 4. Images from a study of motor stimulation involving a hand movement task, obtained with the section positions shown in Figure 1c. **(a)** Anatomy of the superficial plane. **(b)** Activation (associated with right hand movement) in this plane. **(c)** Superimposition of the activated signal (in red) on the anatomic image. **(d–f)** Corresponding images from the middle plane. **(g–i)** Data from the deep plane. For the FLASH images, parameters were 85/60 and pulse angle = 40°. Each activation image was obtained by using seven blocks of control and activation data acquired over a period of 700 seconds. Summation and subtraction were otherwise as performed for Figure 3. Registration of the anatomic images with the activation images was facilitated in some cases by the visualization of blood vessels on both sets of images.

the choice of imaging planes, voxel size, and TE strongly influences the percentage increase in signal intensity that is observed. In the motor activation studies, we were able to show that this increased signal intensity is present in the gray matter of the precentral and postcentral gyri, with little effect in the intervening white matter. Third, our observations were made with a conventional 1.5-T system, with no additional hardware modifications, operating in a routine clinical environment.

The increase in local signal intensity on activation has been attributed primarily to changes in blood oxygenation, in particular to a net conversion of deoxyhemoglobin to oxyhemoglobin (5–8,13). Two observations provide the basis for this explanation. First, it is known that the presence of deoxyhemoglobin can influence signal intensity (because of its paramagnetic iron centers) (13,15,16); most important, it causes gradient-echo signal loss in the vicinity of blood vessels (13). Second, PET studies have shown that during cerebral activity there is an increase in local blood flow with relatively little change in oxygen consumption, so that the venous blood should become more oxygenated on activation (3,4). With this explanation for the signal intensity increase, it has been estimated that visual activation may be expected to produce a 2% signal intensity increase at a field strength of 1.5 T with a TE of 40 msec (5). This translates to a 3% change with the TE of 60 msec used in the present study, which is consistent with our observations at the lower spatial resolution. To what extent this model can account for the much larger (15%) changes observed in our higher-resolution motor activation studies remains to be established. However, it is important to emphasize that these large changes are confined to gray matter. Presumably, this means that the hemodynamic changes on activation occur primarily within the gray matter; therefore, any modeling of the observed effects must consider the blood vessels and hemodynamic changes that are characteristic specifically of the activated gray matter regions. A similar point has previously been made in relation to the observation that the signal intensity changes on visual activation occur predominantly in areas containing gray matter (6,17).

To obtain images of the quality shown in Figures 2–6, we need to time-average the signals, but while this may impose certain limitations on some specific applications in brain physiology and neuroscience, many basic as well as clinical applications are likely to rely more on visualization of functional anatomy than on establishing the detailed time scales of functional activation. Topics of interest include the assessment of functional reorganization following brain injury and preoperative delineation of primary cortical areas.

Behavioral studies show some recovery of basic sensory and motor functions following cortical lesions, particularly if the lesions are sustained in infancy or early childhood (18). For instance, recent observations in cases of infantile hemiplegia (19) show some sparing and/or recovery of function that presumably reflects the plasticity of the immature cerebral cortex. The neural basis of such recov-

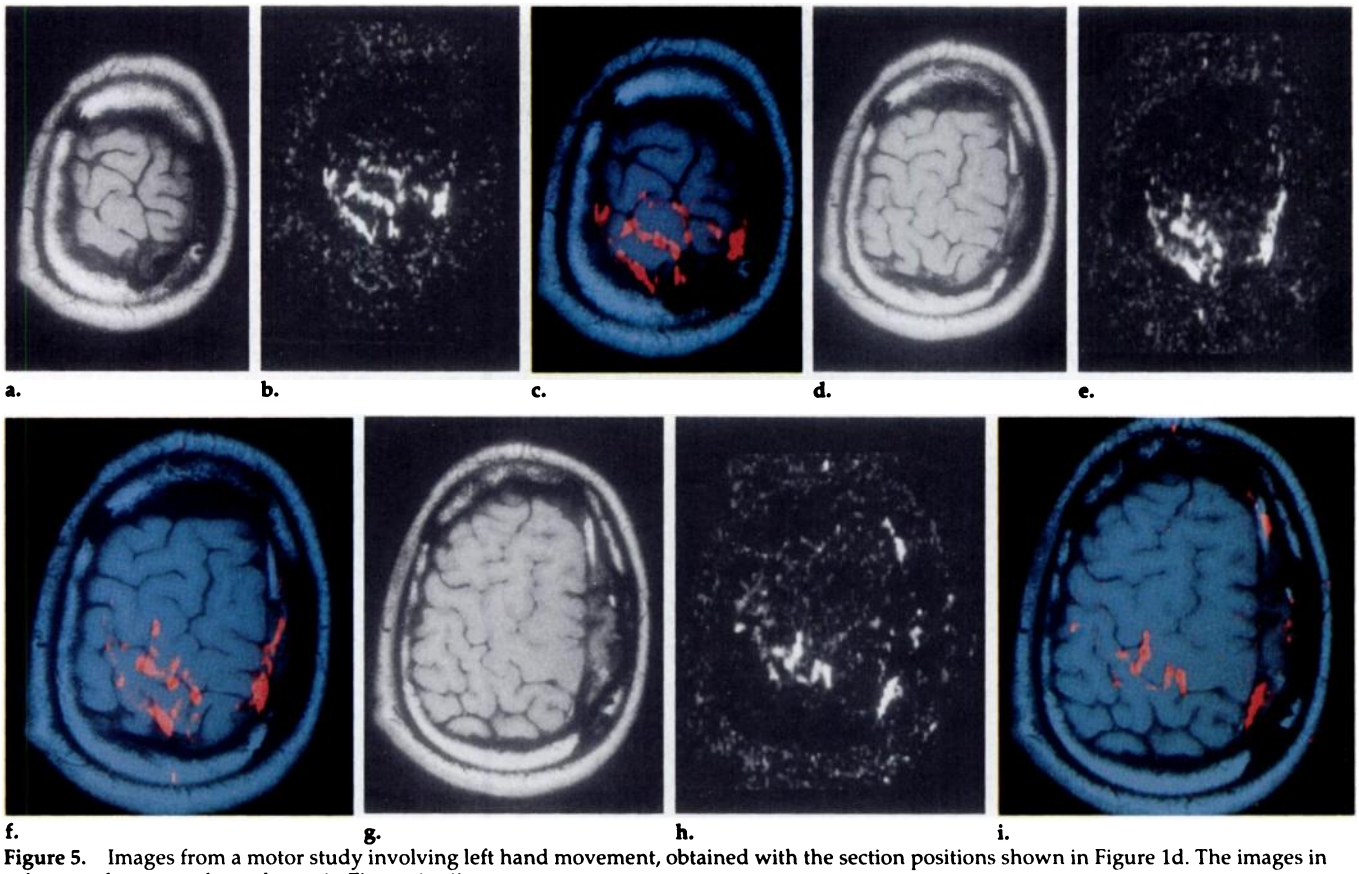

Figure 5. Images from a motor study involving left hand movement, obtained with the section positions shown in Figure 1d. The images in **a–i** are analogous to those shown in Figure 4a–4i.

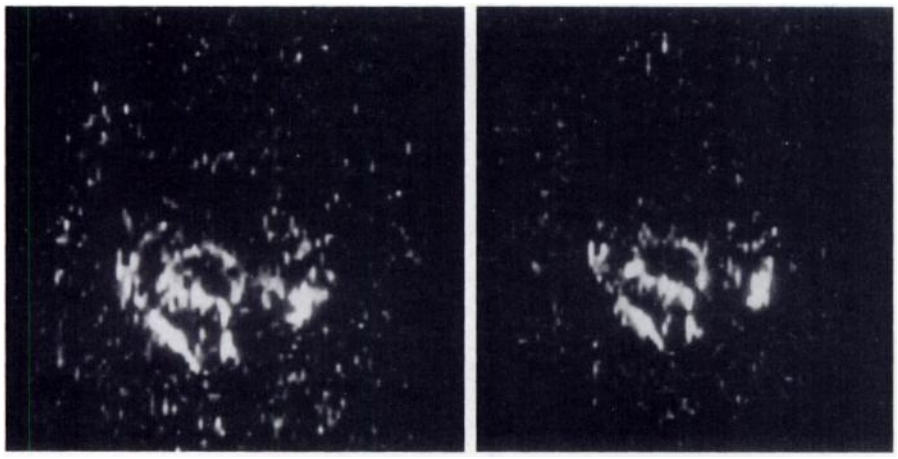

Figure 6. Images from the plane shown in Figure 5a. These activation images were obtained by using one **(a)** and four **(b)** cycles of activity (cf Fig 5b, which was obtained by using seven cycles).

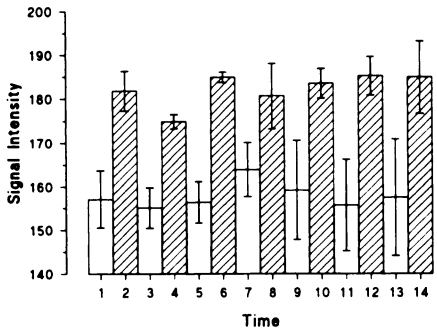

Figure 7. Cyclical signal intensity changes in a region of interest selected from the image shown in Figure 4b. Data are presented as mean ± standard deviation of the signal intensities measured from images 2–5 in each block. Each unit of time represents 50 seconds. Odd-numbered time periods correspond to control values, while even numbers refer to periods of motor activation.

ery is not fully known but, even in adults, there may be functional reorganization of intact cortex, as shown by recent PET studies of patients after stroke (20,21). MR imaging now provides an alternative means of identifying cortical areas that mediate behavioral recovery, both in adults and in children. Functional MR imaging does not use ionizing radiation, can be combined with structural imaging in a single examination, and on the basis of our studies should now become much more widely available. Longitudinal MR imaging studies carried out during the recovery process could be particularly informative.

Functional MR imaging may also have important applications in neurosurgery. Significant morbidity associated with surgical procedures involving the cerebral cortex can result from disruption of primary sensory (visual, auditory, and somatosensory) and motor cortical areas. Neurosurgeons attempting to preserve these primary areas during therapeutic operations are handicapped by variations in the normal organization of these areas as well as by the reorganization that may follow neurologic disease, particularly in children. To overcome this difficulty, intraoperative cortical map-

ping in the awake patient has been used in an attempt to define the extent of a primary area in an individual patient and to allow a decision that balances therapeutic need against potential functional impairment. A routine noninvasive means of identifying the primary area, like that afforded by functional MR imaging, would clearly be of value in clinical management.

In conclusion, we have shown that functional MR imaging of the brain can be carried out with high spatial resolution on a conventional MR imaging system of the type found in many diagnostic radiology departments. We concentrated on visual and motor function, but the degree of activation that we observed during these tasks suggests that other brain systems may also be amenable to study in this manner. The measurements are completely noninvasive, and it is apparent that there will be widespread applications in many areas of neuroscience, clinical neurology, and neurosurgery. ■

Acknowledgments: We thank Nick Geddes for preparation of figures and Duncan Anderson, MBBS, for the use of the goggles.

References

1. Chadwick DJ, Whelan J, eds. Exploring brain functional anatomy with positron tomography. Ciba Found Symp 1991; 163: 1–287.
2. Raichle ME. Circulatory and metabolic correlates of brain function in normal humans. In: The nervous system: higher functions of the brain. Plum F, ed. Bethesda, Md: American Physiological Society, 1987; 643–674.
3. Fox PT, Raichle ME. Focal physiological uncoupling of cerebral blood flow and oxidative metabolism during somatosensory stimulation in human subjects. Proc Natl Acad Sci U S A 1986; 83:1140–1144.
4. Fox PT, Raichle ME, Mintun MA, Dence C. Nonoxidative glucose consumption during focal physiologic neural activity. Science 1988; 241:462–464.
5. Kwong KK, Belliveau JW, Chesler DA, et al. Dynamic magnetic resonance imaging of human brain activity during primary sensory stimulation. Proc Natl Acad Sci U S A 1992; 89:5675–5679.
6. Ogawa S, Tank DW, Menon R, et al. Intrinsic signal changes accompanying sensory stimulation: functional brain mapping with magnetic resonance imaging. Proc Natl Acad Sci U S A 1992; 89:5951–5955.
7. Bandettini PA, Wong EC, Hinks RS, Tikofsky RS, Hyde JS. Time course EPI of human brain function during task activation. Magn Reson Med 1992; 25:390–397.
8. Frahm J, Bruhn H, Merboldt KD, Hänicke W. Dynamic MR imaging of human brain oxygenation during rest and photic stimulation. JMRI 1992; 2:501–505.
9. Blamire AM, Ogawa S, Ugurbil K, et al. Dynamic mapping of the human visual cortex by high-speed magnetic resonance imaging. Proc Natl Acad Sci U S A 1992; 89:11069–11073.
10. Belliveau JW, Kwong KK, Kennedy DN, et al. Magnetic resonance imaging mapping of brain function: human visual cortex. Invest Radiol 1992; 27(suppl):S59–S65.
11. Stehling MK, Turner R, Mansfield P. Echo-planar imaging: magnetic resonance imaging in a fraction of a second. Science 1991; 254:43–50.
12. Haase A, Frahm J, Matthaei D, Hänicke W, Merboldt KD. FLASH imaging: rapid NMR imaging using low flip-angle pulses. J Magn Reson 1986; 67:258–266.
13. Ogawa S, Lee TM. Magnetic resonance imaging of blood vessels at high fields: in vivo and in vitro measurements and image simulation. Magn Reson Med 1990; 16:9–18.
14. Roland PE. Organisation of motor control by the normal human brain. Human Neurobiol 1984; 2:205–216.
15. Brindle KM, Brown FF, Campbell ID, Grathwohl C, Kuchel PW. Application of spin-echo nuclear magnetic resonance to whole-cell systems. Biochem J 1979; 180:37–44.
16. Thulborn KR, Waterton JC, Matthews PM, Radda GK. Oxygenation dependence of the transverse relaxation time of water protons in whole blood at high field. Biochim Biophys Acta 1982; 714:265–270.
17. Belliveau JW, Kennedy DN, McKinstry RC, et al. Functional mapping of the human visual cortex by magnetic resonance imaging. Science 1991; 254:716–719.
18. Teuber HL. Recovery of function after brain injury in man. In: Porter R, Fitzsimons DW, eds. Outcome of severe damage to the central nervous system. Ciba Found Symp 1975; 34:159–190.
19. Farmer SF, Harrison LM, Ingram DA, Stephens JA. Plasticity of central motor pathways in children with hemiplegic cerebral palsy. Neurology 1991; 41:1505–1510.
20. Chollet F, DiPiero V, Wise RJS, Brooks DJ, Dolan RJ, Frackowiak RSJ. The functional anatomy of motor recovery after stroke in humans: a study with positron emission tomography. Ann Neurol 1991; 29:63–71.
21. Weiller C, Chollet F, Friston KJ, Wise RJS, Frackowiak RSJ. Functional reorganization of the brain in recovery from striatocapsular infarction in man. Ann Neurol 1992; 31:463–472.